AAEC/E278

AAEC/E278

AUSTRALIAN ATOMIC ENERGY COMMISSION
RESEARCH ESTABLISHMENT
LUCAS HEIGHTS

PERFORMANCE OF A THERMOSIPHON EVAPORATOR FOR CONCENTRATION OF URANYL NITRATE SOLUTIONS

D.M. LEVINS

P.G. ALFREDSON

May 1973

ISBN 0 642 99565 6

AUSTRALIAN ATOMIC ENERGY COMMISSION

RESEARCH ESTABLISHMENT

LUCAS HEIGHTS

PERFORMANCE OF A THERMOSIPHON EVAPORATOR FOR CONCENTRATION OF URANYL NITRATE SOLUTIONS

by

D. M. LEVINS

P. G. ALFREDSON

ABSTRACT

The performance of a thermosiphon evaporator, with a heat transfer area of 0.74 m^2, for the concentration of uranyl nitrate solutions up to 1000 gU ℓ^{-1} is evaluated. The effects of steam pressure, uranium concentration and liquid submergence on the overall heat transfer coefficient are reported and a method of designing thermosiphon evaporators handling concentrated uranyl nitrate solutions is proposed. Pressure drop characteristics of two packings used in the steam stripping and de-entrainment sections of the evaporator are also given.

Overall heat transfer coefficients in the range 1.4 – 2.5 kW m^{-2} K^{-1} were obtained at uranyl nitrate concentrations up to 1000 gU ℓ^{-1}. Heat transfer to uranyl nitrate solutions below a concentration of 100 gU ℓ^{-1} was satisfactorily predicted by employing conventional heat transfer correlations using physical property data for water. Results for more concentrated solutions were successfully correlated using an empirical correction factor which accounts for the change in physical properties of the boiling solution with concentration.

National Library of Australia card number and ISBN 0 642 99565 6

The following descriptors have been selected from the INIS Thesaurus to describe the subject content of this report for information retrieval purposes. For further details please refer to IAEA–INIS–12 (INIS: Manual for Indexing) and IAEA–INIS–13 (INIS: Thesaurus) published in Vienna by the International Atomic Energy Agency.

CRITICALITY; EVAPORATION; HEAT TRANSFER; PERFORMANCE; PURIFICATION; SAFETY; SOLVENT EXTRACTION; STEAM; URANIUM; URANYL NITRATES

CONTENTS

(continued)

CONTENTS (continued)

1. INTRODUCTION

In uranium refining, dilute solutions must frequently be evaporated before further treatment, for example, when uranium trioxide is produced by the fluidised bed denitration route. The uranyl nitrate from solvent extraction purification with tributyl phosphate typically has a concentration in the range 70–120 gU ℓ^{-1} and must be evaporated up to 1000 gU ℓ^{-1} to produce a suitable feed for thermal denitration.

The vertical tube, thermosiphon evaporator has been used widely in nuclear service (Long 1967, Stoller and Richards 1961). Its advantages are simplicity of construction, flexibility in operation, high overall heat transfer coefficient and small liquid hold-up. Also, this evaporator is best suited for handling enriched uranium and plutonium streams where criticality considerations pose severe restrictions on evaporator geometry (Lindley 1963, Klitgaard et al. 1964).

This report gives details of the performance of a vertical tube, thermosiphon evaporator for producing concentrated uranyl nitrate solutions suitable for denitration. The effects of steam pressure, uranium concentration and liquid submergence on the heat flux and overall heat transfer coefficient are reported and a method of designing thermosiphon evaporators handling concentrated uranyl nitrate solutions is proposed. Pressure drop characteristics of two packings used in the steam stripping and de-entrainment sections of the evaporator are also given.

2. EQUIPMENT

Figure 1 shows the evaporator unit and an equipment flowsheet is given in Figure 2. The principal components of the unit are the boiler, disengagement section, return leg, steam stripping and de-entrainment columns, and the condenser. All parts in contact with uranyl nitrate or nitric acid solutions are of AISI 304L stainless steel.

The vertical tube boiler is 168 mm in diameter, 1.22 m long and has 7 tubes of one inch Schedule 10 (28 mm i.d.) pipe giving an inner heat transfer area of 0.74 m^2. Uranyl nitrate solution is heated by steam supplied at a controlled pressure to the shell side of the heat exchanger.

A section of enlarged cross-section (460 mm dia. x 530 mm long) is located immediately above the boiler to allow for disengagement of the gas-liquid mixture generated by the boiling action. Boiler glass windows are provided in the disengagement section to observe the operation and to detect any tendency towards foaming. A return leg of 50 mm diameter beginning at the base of the disengagement section allows for liquid recirculation to the bottom of the boiler induced by the difference in densities between the boiling and non-boiling solutions.

Steam from the evaporator passes through a 125 mm dia. x 760 mm long packed column where it contacts the feed solution countercurrently. The purpose of this steam stripping section is to preheat the feed and remove any traces of organic solvent before it enters the evaporator. If the feed liquid passed directly to the evaporator, a possibility exists of an explosion caused by nitration of the solvent (Colven et al. 1953).

Above the feed point is a further 125 mm dia. packed column, 610 mm long (following the work of Bell and Grimley 1960). This 'de-entrainment section' is designed to knock out any droplets of feed solution that become entrained in the vapour stream. Vapour emerging from the de-entrainment section is condensed in a double pipe condenser, 50 mm in diameter and 2.20 m long with an outer heat transfer area of 0.35 m^2. The condensate which is a dilute nitric acid solution is collected in a 0.2 m^3 drum which is vented through a caustic bubbler to remove any nitrous fumes.

3. OPERATION AND CONTROL

3.1 Steam and Cooling Water Supply

Steam for the evaporator was supplied at a mains gauge pressure of 800 kPa and was regulated over the range 0–200 kPa as required. A pressure release valve set to operate at 200 kPa ensured that mains pressure could never be applied to the boiler. As a further safety measure, a solenoid valve in the steam supply line was set to shut off the steam if the liquid temperature in the boiler exceeded 125°C. A valve in the condensate line allowed the shell to be periodically purged of air.

Cooling water was metered to the condenser from a recirculating supply linked to a cooling tower. The maximum flow rate obtainable through the condenser was 0.5 $\ell\ s^{-1}$. Except at the highest evaporation rate, this was sufficient to condense and substantially sub-cool all the vapour from the evaporator.

3.2 Instrumentation and Control

Figure 2 shows the extent of instrumentation and control. All controls are manual except the automatic steam shut-off which operates if the boiling liquid temperature exceeds 125°C.

Liquid density was measured in the return leg of the evaporator by measuring the pressure differential between air purged dip tubes. Two tubes 75 mm apart near the base of the return leg allowed density to be read directly using a 'Magnehelic' differential pressure gauge. Uranyl nitrate concentration can be determined from the density measurement (see Figure 3). Solution density is also affected by nitric acid concentration but with the relatively dilute acid feed streams employed (typically 0.05M HNO_3) no correction for nitric acid concentration was necessary. Uranyl nitrate concentrations determined by gamma absorptiometry (Yates and May 1970) and from Figure 3 generally agreed within 10–15 g ℓ^{-1}.

Density measurements were most accurately obtained by switching off the steam briefly before a reading was taken. Pressure drop readings tended to fluctuate periodically during operation and were generally lower than those obtained under static conditions. The low readings during operation were attributed to the frictional pressure drop due to liquid recirculation and to entrainment of steam into the return leg.

Liquid level was determined in the return leg by measuring the differential pressure between the base of the return leg and the vapour space above the evaporator. This does not give the level directly, but rather the product of the liquid level and density. From measurements of the density, the true liquid level can be calculated.

Pressure drops across the steam stripping and de-entrainment columns were measured by air purged 'Magnehelic' gauges with full scale deflections corresponding to 1.2 kPa. Temperature was measured and recorded by thermocouples inserted at various points in the evaporator and in the condenser cooling water circuit.

3.3 Safety

Under certain circumstances, tributyl phosphate (TBP) will react explosively with nitric acid or uranyl nitrate solutions or combinations of both. A violent explosion did, in fact, occur in an evaporator at Savannah River in 1953 while a UNH-HNO_3-TBP mixture was being concentrated. Following the incident, experiments were performed to establish the conditions under which reaction could occur (Colven et al. 1953). It was found that TBP must be present in concentrations well above its solubility in water (0.3 g ℓ^{-1}) for an explosion to occur and then a temperature above 135°C was also required. It was recommended that to ensure safe operation, TBP in excess of water soluble quantities must not be permitted to enter the evaporator and liquid temperatures should be maintained below 125°C.

The following measures were taken to ensure that an explosion was not possible in the evaporator.

(1) Steam gauge pressure was limited by a pressure release valve to 200 kPa. This corresponds to a maximum temperature on the steam side of the boiler of 135°C.

(2) A contact thermometer immersed in the boiling liquid was set to close a solenoid valve on the steam supply line should the temperature rise to 125°C.

(3) The evaporator was designed with a steam stripping section to prevent even water soluble amounts of TBP from entering the evaporator.

(4) The tank supplying uranyl nitrate feed was never completely drained so that TBP which may have settled on top of the aqueous layer could not be passed into the evaporator.

3.4 Operational Procedure

The evaporator unit was designed for batch operation producing concentrated uranyl nitrate solutions from a feed of 70–120 gU ℓ^{-1}. The standard product batch size was 35 ℓ of 570 gU ℓ^{-1} although 55 ℓ batches of up to 1000 gU ℓ^{-1} could be produced if required.

A production run commenced by adding demineralised water to the evaporator approximately to the 20 ℓ level and adjusting the regulator to deliver steam at a pressure not greater than 170 kPa. When boiling commenced, cooling water was supplied to the condenser, the feed valve was opened and dilute uranyl nitrate was metered to the evaporator at a rate of about 40 ℓ h^{-1}. Steam pressure was then adjusted so that the pressure drop over the stripping column did not exceed 0.9 kPa which was about 50% of the value at the loading point. The feed rate to the evaporator was adjusted periodically so that the liquid remained at a required level. As the product concentration was approached, the evaporation rate decreased. The steam pressure was then increased to maintain the pressure drop over the stripping section at about 0.9 kPa and to restore the evaporation rate to its steady value. When the density and level indicators showed that the required concentration and quantity of uranyl nitrate had been reached, the steam and cooling water supply valves were closed and the concentrated liquor was pumped from the evaporator.

4. EXPERIMENTAL

4.1 Heat Transfer Measurements

The usual procedure was to set the desired steam pressure and adjust the liquid level and density to the required values. In most cases water was fed to the unit at a rate which approximated that of evaporation so that the original liquid level and concentration was maintained throughout the run. After steady state conditions had been established, the time required for a specific quantity, usually 2–10 ℓ, of condensate to be collected was measured. The overall heat transfer rate, Q, was calculated from the condensate flow rate V and the liquid rate F.

$$Q = V\lambda + Fc_p(T_b - T_f) + L \quad . \tag{1}$$

Heat losses L through the insulated sections of the unit were calculated to be approximately 0.6 kW.

Heat transfer coefficients were calculated from the equation,

$$U_i = \frac{Q}{A_i(T_s - T_b)} \quad , \tag{2}$$

where A_i is the tubeside surface area (0.74 m^2), T_s is the temperature of the condensing steam assumed saturated at the supply pressure and T_b is the boiling point of solution at the pressure in the vapour space above the boiler (essentially atmospheric). The boiling point rise for uranyl nitrate-nitric acid solutions was taken from the data of Lane (1945) which is presented in Figure 4. In accordance with usual practice, the calculated heat transfer coefficient was not corrected for the effect of static liquid level.

When water was evaporated at high steam pressures, the capacity of the condenser was unable to match that of the boiler and only part of the vapour condensed. In these cases, the evaporation rate was determined from the change in liquid level in the evaporator.

In all, sixty-six determinations of heat transfer rate were made for gauge steam pressures ranging from 41–205 kPa and for uranium concentrations from 0–1000 gU ℓ^{-1}. Results are shown in Tables 1–6.

4.1.1 Effect of steam pressure

Figure 5 shows the variation of the rate of heat transfer with steam pressure. Heat flux varies approximately linearly with steam pressure for uranyl nitrate solutions, but the results for water over an extended range show some curvature. Of more fundamental interest is the comparison between the overall heat transfer coefficient and the temperature differential across the heat exchanger (Figure 6). For small differential temperatures (< 15 K) the heat transfer coefficient is markedly dependent on ΔT, but above 20 K the coefficient is approximately constant.

4.1.2 Effect of uranyl nitrate concentration

As shown in Figure 5, uranyl nitrate concentration has a marked effect on the evaporative capacity of the boiler. At a steam gauge pressure of 100 kPa, for example, the heat transfer rate to 750 gU ℓ^{-1} solution is only about one-fifth of the rate to water. But when allowance is made for the boiling point elevation of uranyl nitrate solutions, as in Figure 6, the effect of concentration is not as evident. For a temperature drop across the boiler of 15 K, for example, the overall heat transfer coefficient for 750 gU ℓ^{-1} solution is only 20 per cent below the figure for water.

4.1.3 Effect of liquid submergence

The effect of liquid submergence (defined here as the percentage of heat exchanger surface covered by liquid under static or non-boiling conditions) on evaporation performance was studied using water. The results, which are shown in Figure 7, indicate only a slight increase in evaporative capacity as submergence is decreased. Below 20 per cent submergence, the heat transfer rate fell away sharply. This lack of sensitivity of evaporative capacity to submergence is unusual since heat transfer is generally reported to be affected strongly by submergence and to attain a maximum at about 50 per cent (Perry 1963). It appears that circulation in the evaporator was not much affected by submergence except below 20 per cent when circulation was not achieved. Operation and control were more satisfactory at complete submergence and all production runs were carried out under these conditions.

4.1.4 Condenser performance

The heat removal capacity of the condenser was 33 kW at a cooling water flow rate of 1.5 $m^3\,h^{-1}$ and 39 kW at 2.2 $m^3\,h^{-1}$. These figures correspond to heat transfer coefficients in the range 1.5 – 1.8 $kW\,m^{-2}\,K^{-1}$ and are consistent with published data for similar systems (Kern 1950, Perry 1963), having regard for the relatively low cooling water velocities obtainable (0.5 – 0.7 $m\,s^{-1}$) in the annular jacket.

For uranium concentrations below 500 g ℓ^{-1}, the condenser capacity now limits the overall performance of the unit. If it were considered desirable to uprate the duty of the unit, this could best be achieved by replacing the present double pipe condenser with a shell and tube heat exchanger.

4.2 Pressure Drop Measurements

Two types of packing were tested in the steam stripping and de-entrainment sections of the evaporator. Initially these sections were packed with 9.5 mm glass Raschig rings but the pressure drop was so high that flooding occurred at relatively low evaporation rates (30 $\ell\,h^{-1}$).

These were replaced with 16 mm glass Raschig rings which extended the range of the unit further but flooding still took place at the highest evaporation rates (45 ℓ h^{-1}). As it is generally recommended that the ratio of column to packing diameter should be greater than 7 (Peters and Timmerhaus 1968), it was decided to use a wire packing rather than Raschig rings of still larger diameter.

Figure 8 compares the pressure drop characteristics of 16 mm dia. glass Raschig rings and 'Springmesh' PSA/10/W/6, a stainless steel knitted mesh packing with a density of 200 kg m^{-3}. Three of the four curves are for no liquid flow, the fourth shows the pressure drop for a liquid loading of 1.63 kg m^{-2} s^{-1}. In the last case, the water feed was heated almost to the boiling point to eliminate condensation effects. For the same steam velocity, the pressure drop for the mesh packing was considerably lower. Because of this, 'Springmesh' packing has been installed permanently in the column.

5. DISCUSSION

5.1 Individual Heat Transfer Coefficients

The overall resistance to heat transfer in an evaporator is the resultant of a number of resistances in series viz.,

(1) a resistance through a film of condensate on the shell side, r_s;

(2) resistance through the tube wall, r_m;

(3) a resistance at the boiling surface, r_b;

(4) any fouling resistances, r_{fo}, r_{fi} arising from scale deposits on either side of the boiler

$$R = r_s + r_m + r_b + r_{fo} + r_{fi} \quad . \tag{3}$$

Equation (3) is more commonly expressed in terms of individual heat transfer coefficients, viz.,

$$\frac{1}{U_i} = \frac{A_i}{A_o h_s} + r_m + \frac{1}{h_b} + r_{fo} + r_{fi} \quad . \tag{4}$$

The heat transfer coefficient for condensing steam can be calculated accurately from the theoretical expression for conduction through a falling liquid film,

$$h_s = \frac{4}{3}\left[\frac{\pi n_t D_o \lambda k^3 \rho^2 g}{3 \mu Q}\right]^{1/3} . \tag{5}$$

The physical properties in equation (5) refer to those of the liquid at the mean film temperature.

The wall resistance is given by,

$$r_m = \frac{2.3 D_i}{2 k_m} \log \frac{D_o}{D_i} \quad . \tag{6}$$

For tubes with thick walls of a low thermal conductivity material, such as stainless steel, this resistance can be appreciable.

Heat transfer to boiling liquids is a complex phenomenon whose mechanism has not been clearly established despite extensive research. When the temperature difference between surface and liquid is very low, heating occurs by natural convection. As the temperature difference is increased, bubbles form and break away from active sites on the surface and the heat transfer rate increases significantly. This is the nucleate boiling region in which most industrial evaporators and reboilers operate. For very large differential temperatures, a continuous film of vapour is formed which blankets the surface and the heat transfer rate drops away.

Heat transfer by nucleate boiling is a function of the physical properties of the solution, the temperature difference between surface and solution and other factors which are less easily described mathematically viz., the hydrodynamics of two-phase flow and the nature and condition of the heat transfer surface. In a rigorous analysis of a thermosiphon evaporator, the calculation of heat transfer rate is combined with the hydrodynamics of the equipment in an iterative calculation to determine the circulating rate through the reboiler (Kern 1950, McKee 1970, Hughmark 1969). The local heat transfer coefficient can then be evaluated from equations for forced convection heat transfer and the average heat transfer coefficient calculated by integration along the tube length. Such an approach is extremely laborious and is usually not justified when viewed against the uncertainties in our understanding of the mechanism involved (Lord et al. 1970).

The most widely quoted equation for nucleate boiling is that of Gilmour (1958, 1959);

$$\frac{h_b}{c_p G} = \phi\, \alpha \left(\frac{D_i G}{\mu}\right)^{-0.3} \left(\frac{c_p \mu}{k}\right)^{-0.6} \left(\frac{\rho_L \sigma}{P^2}\right)^{-0.43} , \qquad (7)$$

where

$$G = \frac{Q}{\lambda A_i}\left(\frac{\rho_L}{\rho_v}\right) , \qquad (8)$$

and ϕ = metal type factor (0.001 for copper and steel, 0.00059 for stainless steel), α = surface condition factor (1.0 for perfectly clean conditions, 1.7 for average tube conditions, 2.5 for worst tube conditions).

The fouling resistances, r_{fo} and r_{fi} are a function of time, the fluid characteristics and flow conditions and the type of surface. Recommended values for typical conditions encountered in the process industry are available (TEMA 1959).

5.2 Prediction of Heat Transfer Rates

Equations (4) to (8) can be used to predict individual and overall heat transfer coefficients. In applying these equations, the values α = 1.0, r_{fo} = r_{fi} = 0 have been chosen since the measurements of heat transfer rate were made soon after the unit began operation. Figure 9 shows the predicted coefficients for water as a function of the heat flux. All three resistances play a significant role in determining the overall heat transfer coefficient. The resistance at the boiling surface predominates at the lower heat fluxes, the wall resistance contributes most in the intermediate region while the resistance through the film of condensate on the steam side is most important at the highest evaporation rates.

Predicted and measured values of the overall coefficient using water are shown in Figure 10. Both follow the same trend; for low values of heat flux, the overall coefficient increases sharply at first as heat flux is increased but levels off to an almost constant value at the highest evaporation rates. The average deviation of measured coefficients from those predicted is only 6 per cent.

The same approach could be applied to uranyl nitrate solutions if the relevant physical property data for use in equation (7) were available. According to equation (7), h_b varies with the physical properties of the boiling liquid as follows,

$$h_b \propto \frac{\rho_L^{0.27}\, c_p^{0.40}\, k^{0.60}}{\sigma^{0.43}\, \mu^{0.30}} . \qquad (9)$$

Unfortunately no data have been reported for the thermal conductivity and surface tension of uranyl nitrate solutions and the available viscosity data must be extrapolated outside the reported range (Slansky 1958). Of the other factors, ρ_L increases and c_p decreases (Krigens 1968) as uranyl nitrate concentration increases. Overall, h_b decreases as concentration increases mainly because of the rise in viscosity.

It is possible to estimate the value of h_b for uranyl nitrate solutions from measured values of the overall coefficient and equations (4)–(6). When this is done it is found that heat transfer coefficients for uranyl nitrate solutions can be expressed by the equation,

$$h_b = f(C)\, h_{bw} \quad , \tag{10}$$

where h_{bw} is the value for water under the same conditions and f(C) is a factor which accounts for the change in physical properties with concentration. Comparing equations (9) and (10) gives,

$$f(C) = \left(\frac{\rho_L}{\rho_{Lw}}\right)^{0.27} \left(\frac{c_p}{c_{pw}}\right)^{0.40} \left(\frac{k}{k_w}\right)^{0.60} \left(\frac{\sigma_w}{\sigma}\right)^{0.43} \left(\frac{\mu_w}{\mu}\right)^{0.30} \quad . \tag{11}$$

Because values for k, σ and μ were not known with sufficient accuracy, equation (11) cannot be used to determine f(C).

Figure 11 shows a plot of f(C) against uranyl nitrate concentration derived from the experimental data with only average values of f(C) shown on the graph. The relationship between f(C) and concentration C is most simply represented by

$$f(C) = 1 - 6.2 \times 10^{-4}\, C \quad , \tag{12}$$

where C is expressed as gU ℓ^{-1}.

5.3 Comparison with Previous Work

Only a few measurements of heat transfer coefficients for boiling uranyl nitrate solutions have been reported, mostly on a limited scale (Table 7). All reported results cover roughly the same range. The data of Klitgaard et al. (1964) are the most extensive and are most easily compared with the results reported here. Both Klitgaard's work and the present results show the same trend; heat transfer coefficients at first increase as steam pressure is raised but eventually reach a plateau. Table 8 shows the maximum value in the plateau region as a function of uranium concentration. Klitgaard's results are about 10 per cent higher than those of the present work. The difference in tube wall thickness (2 mm in Klitgaard's work and 2.8 mm for this work) is sufficient to account for this discrepancy.

6. DESIGN OF THERMOSIPHON EVAPORATORS FOR CONCENTRATING URANYL NITRATE SOLUTIONS

The following procedure is recommended for designing vertical thermosiphon evaporators.

(1) Determine the required heat duty.

(2) Set the operating steam pressure. If the feed uranyl nitrate solution arises from solvent extraction with tributyl phosphate, the gauge steam pressure should be limited to 200 kPa to safeguard against possible explosions.

(3) Estimate an overall coefficient from Figure 6. Calculate the required heat transfer area from equation (2).

(4) Decide on a tentative tube layout and the length of the tube bundle. Typical tube diameters range from 25–40 mm with tube lengths from 1 to 3 m.

(5) Calculate the steam side heat transfer coefficient from equation (5).

(6) Having selected the minimum wall thickness consistent with the design pressure and expected corrosion rate, calculate the wall resistance using equation (6).

(7) Determine the boiling heat transfer coefficient for water from equation (7). Adjust for the maximum product concentration of uranyl nitrate using equations (10) and (12).

(8) Estimate fouling resistances, r_{fo} and r_{fi}. In the absence of any other data the values $r_{fo} = r_{fi} = 0.15\ m^2\ K\ kW^{-1}$ are recommended.

(9) If a packed column is to be employed for steam stripping or de-entrainment purposes, it should be sized so that the pressure drop does not exceed 1 kPa/m packing. A robust packing such as Raschig rings is probably preferable to wire mesh for a long service life in a production evaporator. The required column diameter can then be calculated from Figure 8 or the literature (Perry 1963).

7. CONCLUSIONS

(1) Overall heat transfer coefficients in the range 1.4 – 2.5 $kW\ m^{-2}\ K^{-1}$ have been obtained in a vertical thermosiphon evaporator at uranyl nitrate concentrations of up to 1000 $gU\ \ell^{-1}$.

(2) For small differential temperatures across the boiler (< 15 K), the overall heat transfer coefficient was markedly dependent on ΔT, but was approximately constant for temperature differences above 20 K.

(3) Heat transfer to uranyl nitrate solutions below a concentration of 100 $gU\ \ell^{-1}$ was satisfactorily predicted by employing conventional heat transfer correlations using physical property data for water. Results for more concentrated solutions were successfully correlated using an empirical correction factor which accounted for the change in physical properties of the boiling solution with concentration.

(4) The submergence of liquid in the heat exchanger section had only a minor effect on the evaporative capacity.

8. ACKNOWLEDGEMENTS

The authors acknowledge the assistance of many members of Chemical Engineering Section in the course of this work, particularly Mr. R. C. Hirst who was involved in the initial design of the evaporator, and Mr. H. Romyn who carried out most of the experimental work. The authors are also grateful to Messrs. B. G. Charlton and V. Vilkaitis and their co-workers who provided the uranyl nitrate feed solutions.

9. REFERENCES

Bell, B.T. and Grimley, S.S. (1960). – Capacity, control and TBP steam stripping trials in a small evaporator. AERE–R 3508.

Colven, T.J., Nichols, G.M. and Siddall, T.H. (1953). – Interim technical report, TNX evaporator incident, January 12, 1953, DP–25.

Gilmour, C.H. (1958). – Nucleate boiling: a correlation. Chem. Eng. Progr. 54 (10): 77–79.

Gilmour, C.H. (1959). – Performance of vaporizers, heat transfer analysis of plant data. Chem. Eng. Progr. Symp. Series 55 (29): 67–78.

Hughmark, G.A. (1969). – Designing thermosiphon reboilers. Chem. Eng. Progr. 65 (7): 67–70.

Kern, D.Q. (1950). – Process Heat Transfer, McGraw Hill, New York.

Klitgaard, J., Geens, L., Van Bijlen, H. and Redon, A, (1964). – Experiments carried out on the Eurochemic testing station climbing-film evaporator. ETR–160.

Krigens, A.G. (1968). – A compilation of physical and chemical properties of materials and streams encountered in the chemical processing department. ARH–724 ADD.

Lane, J.A. (ed.) (1945). – Project handbook Vol. 1. Physical and chemical properties, USAEC Report CL–697.

Lindley, J. (1963). – Titanium evaporator for uranium and plutonium liquors. Brit. Chem. Eng. 8 (6): 397–400.

Long, J.T. (1967). – Engineering for Nuclear Fuel Reprocessing. Gordon and Breach, New York.

Lord, R.C., Minton, P.E. and Slusser, R.P. (1970). – Design of heat exchangers. Chem. Eng. 77 (2): 96–118.

McKee, H.R. (1970). – Thermosiphon reboilers: a review. Ind. Engng. Chem. 62 (12): 76–82.

Perry, J.H. (1963). – Chemical Engineers' Handbook, 4th edn, McGraw Hill, New York.

Peters, M.S. and Timmerhaus, K.D. (1968). – Plant Design and Economics for Chemical Engineers, 2nd edn, McGraw Hill, New York.

Slansky, C.M. (1958). – Physical properties of uranyl nitrate, aluminium nitrate, nitric acid and water system in Bruce, F.R., Fletcher, J.M. and Hyman, H.H. (eds). – Progress in Nuclear Energy Series III. Process Chemistry Vol. 2: 535–43, Pergamon Press, London.

Stoller, S.M. and Richards, R.B. (1961). – Reactor Handbook. Vol. II Fuel Reprocessing, 2nd edn, Interscience, New York.

TEMA (1959). – Standards of Tubular Exchanger Manufacturers' Association Inc., New York, 4th edn.

Yates, P.B. and May, J.R. (1970). – An instrument for analysis of natural uranium solutions by gamma absorptiometry AAEC/TM557.

10. NOMENCLATURE

A = heat transfer area

C = uranyl nitrate concentration

c_p = specific heat

D = tube diameter

F = feed rate

G = mass velocity of liquid (see equation (8))

g = acceleration due to gravity

h = individual heat transfer coefficient

k	=	thermal conductivity
L	=	heat losses through insulation
n_t	=	number of tubes
P	=	pressure
Q	=	heat transfer rate
R	=	overall resistance to heat transfer
r	=	individual resistance to heat transfer
r_{fi} , r_{fo}	=	inside and outside fouling factors
T	=	temperature
U	=	overall heat transfer coefficient
V	=	vapour flow rate
α	=	surface condition factor
λ	=	latent heat of vaporisation
μ	=	absolute viscosity
ρ	=	density
σ	=	surface tension
ϕ	=	metal type factor

Subscripts

b	=	boiling
f	=	feed
i	=	inside
L	=	liquid
m	=	metal
o	=	outside
s	=	steam-side
V	=	vapour
w	=	water

TABLE 1

HEAT TRANSFER COEFFICIENTS

Boiling Liquid – Water Submergence – 100%

Run	Steam Gauge Pressure (kPa)	Steam Temperature (°C)	Vapour Flow V(ℓ h^{-1})	Liquid Feed Rate F(ℓ h^{-1})	Heat Flow Q(kW)	ΔT (K)	U (kW m^{-2} K^{-1})
W–1	41	109.5	14.8	0	9.9	9.5	1.41
W–2	41	109.5	12.5	16	9.9	9.5	1.41
W–3	44	110.2	17.0	0	11.2	10.2	1.48
W–4	54	112.2	25.4	0	16.5	12.2	1.83
W–5	54	112.2	20.0	21	15.1	12.2	1.67
W–6	68	114.9	31.4	25	22.6	14.9	2.05
W–7	68	114.9	34.0	31	24.8	14.9	2.25
W–8	68	114.9	35.9	0	23.1	14.9	2.09
W–9	81	117.1	45.2	0	28.9	17.1	2.28
W–10	81	117.1	42.8	39	31.1	17.1	2.46
W–11	95	119.4	53.6	0	34.2	19.4	2.38
W–12	109	121.6	60.0	0	38.2	21.6	2.39
W–13	122	123.6	68.2	0	43.4	23.6	2.49
W–14	136	125.6	73.7	0	46.8	25.6	2.47
W–15	150	127.5	78.0	0	49.5	27.5	2.43
W–16	163	129.1	82.8	0	52.5	29.1	2.44

TABLE 2

HEAT TRANSFER COEFFICIENTS

Boiling Liquid – Uranyl Nitrate 200 gU ℓ^{-1}, Nitric Acid 0.11 M (b.p. = 101.7 °C)
Submergence 100%

Run	Steam Gauge Pressure (kPa)	Steam Temperature (°C)	Vapour Flow $V(\ell\ h^{-1})$	Liquid Feed Rate $F(\ell\ h^{-1})$	Heat Flow $Q(kW)$	ΔT (K)	U $(kW\ m^{-2}\ K^{-1})$
U–1	48	111.0	9.7	11.5	7.8	9.3	1.13
U–2	54	112.2	13.0	28.5	11.4	10.5	1.47
U–3	61	113.5	18.7	18.7	14.1	11.8	1.61
U–4	68	114.9	21.9	21.5	16.3	13.2	1.67
U–5	68	114.9	21.8	36.0	17.6	13.2	1.81
U–6	75	116.1	29.4	26.4	21.4	14.4	2.01
U–7	75	116.1	26.2	20.5	19.0	14.4	1.78
U–8	82	117.2	31.1	42.4	24.1	15.5	2.10
U–9	88	118.3	38.0	34.0	27.6	16.6	2.24
U–10	95	119.4	37.2	45.7	28.2	17.7	2.15
U–11	102	120.5	42.2	40.2	30.8	18.8	2.21

TABLE 3

HEAT TRANSFER COEFFICIENTS

Boiling Liquid – Uranyl Nitrate 505 gU ℓ^{-1}, Nitric Acid 0.7 M (b.p. = 106.8°C)
Submergence 100%

Run	Steam Gauge Pressure (kPa)	Steam Temperature (°C)	Vapour Flow V(ℓ h^{-1})	Liquid Feed Rate F(ℓ h^{-1})	Heat Flow Q(kW)	ΔT (K)	U (kW m^{-2} K^{-1})
U–13	68	114.9	6.6	10.1	5.8	8.1	0.97
U–14	68	114.9	6.9	9.1	5.8	8.1	0.97
U–15	75	116.1	9.4	12.4	7.7	9.3	1.12
U–16	82	117.2	13.6	15.0	10.6	10.4	1.38
U–17	88	118.3	15.1	15.2	11.6	11.5	1.37
U–18	95	119.4	17.5	19.0	13.4	12.6	1.44
U–19	102	120.5	22.3	22.0	16.8	13.7	1.65
U–20	109	121.6	28.9	21.0	20.7	14.8	1.89
U–21	109	121.6	27.2	26.4	20.3	14.8	1.85
U–22	122	123.6	31.3	33.0	23.5	16.8	1.90
U–23	129	124.6	36.5	35.2	27.0	17.8	2.05
U–24	136	125.6	38.8	41.0	29.0	18.8	2.09
U–25	140	126.1	40.2	40.2	29.7	19.3	2.08
U–26	150	127.5	41.4	49.0	31.4	20.7	2.06

TABLE 4

HEAT TRANSFER COEFFICIENTS

Boiling Liquid – Uranyl Nitrate 750 gU ℓ^{-1}, Nitric Acid 0.35 M (b.p. 110.8°C)
Submergence 100%

Run	Steam Gauge Pressure (kPa)	Steam Temperature (°C)	Vapour Flow V(ℓ h^{-1})	Liquid Feed Rate F(ℓ h^{-1})	Heat Flow Q(kW)	ΔT (K)	U (kW m^{-2} K^{-1})
U–27	78	116.7	3.1	2.8	2.8	5.9	0.64
U–28	95	119.4	7.7	12.5	6.7	8.6	1.05
U–29	112	122.1	11.6	16.5	9.6	11.3	1.15
U–30	130	124.7	20.2	21.0	15.4	13.9	1.50
U–31	130	124.7	20.7	28.0	16.5	13.9	1.61
U–32	142	126.3	24.4	26.0	18.6	15.5	1.62
U–33	166	129.5	35.8	31.5	26.3	18.7	1.90

TABLE 5

HEAT TRANSFER COEFFICIENTS

Boiling Liquid – Uranyl Nitrate 1000 gU ℓ^{-1}, Nitric Acid 1.2 M (b.p. = 119.4°C)
Submergence 100%

Run	Steam Gauge Pressure (kPa)	Steam Temperature (°C)	Vapour Flow V(ℓ h^{-1})	Liquid Feed Rate F(ℓ h^{-1})	Heat Flow Q(kW)	ΔT (K)	U (kW m^{-2} K^{-1})
U–34	170	130.0	10.5	14.0	8.7	10.6	1.11
U–35	187	132.0	15.0	15.0	11.7	12.6	1.25
U–36	205	134.1	21.0	21.0	15.9	14.7	1.46

TABLE 6

HEAT TRANSFER COEFFICIENTS – EFFECT OF SUBMERGENCE

Boiling Liquid – Water

Run	Steam Gauge Pressure (kPa)	Steam Temperature (°C)	Vapour Flow V(ℓ h^{-1})	Liquid Feed Rate F(ℓ h^{-1})	Heat Flow Q(kW)	ΔT (K)	U (kW m^{-2} K^{-1})
			Submergence – 25%				
W–17	41	109.5	17.4	19.5	13.3	9.5	1.89
W–18	65	114.3	31.2	29.5	22.8	14.3	2.16
W–19	88	118.3	43.3	41.7	31.6	18.3	2.33
			Submergence – 50%				
W–20	41	109.5	13.0	15.0	10.1	9.5	1.44
W–21	65	114.3	28.3	28.0	21.0	14.3	1.99
W–23	88	118.3	42.7	39.6	31.0	18.3	2.29
			Submergence –75%				
W–24	41	109.5	18.0	17.0	13.4	9.5	1.91
W–25	65	114.3	29.1	28.0	21.4	14.3	2.02
W–26	88	118.3	40.8	37.2	29.7	18.3	2.19
W–27	88	118.3	39.2	38.0	28.6	18.3	2.11
			Submergence – 100%				
W–28	41	109.5	11.0	14.5	8.9	9.5	1.27
W–29	65	114.3	27.9	27.0	20.5	14.3	1.94
W–30	88	118.3	39.2	34.0	28.3	18.3	2.09

TABLE 7

REPORTED VALUES OF OVERALL HEAT TRANSFER COEFFICIENTS FOR URANYL NITRATE SOLUTIONS IN THERMOSIPHON EVAPORATORS

Concentration gU ℓ^{-1}	Overall Coefficient kW m^{-2} K^{-1}	Reference
0–520	1.08 – 2.66	Klitgaard et al. (1964)
420	0.96 – 2.71	Stoller and Richards (1961)
100–500	1.08 – 1.84	Lindley (1963)
0–1000	0.64 – 2.49	This work

TABLE 8

MAXIMUM HEAT TRANSFER COEFFICIENTS AS A FUNCTION OF URANYL NITRATE CONCENTRATION

Concentration gU ℓ^{-1}	Klitgaard et al. (1964) kW m^{-2} K^{-1}	This Work kW m^{-2} K^{-1}
0	2.66	2.46
200	2.54	2.26
505	2.45	2.09

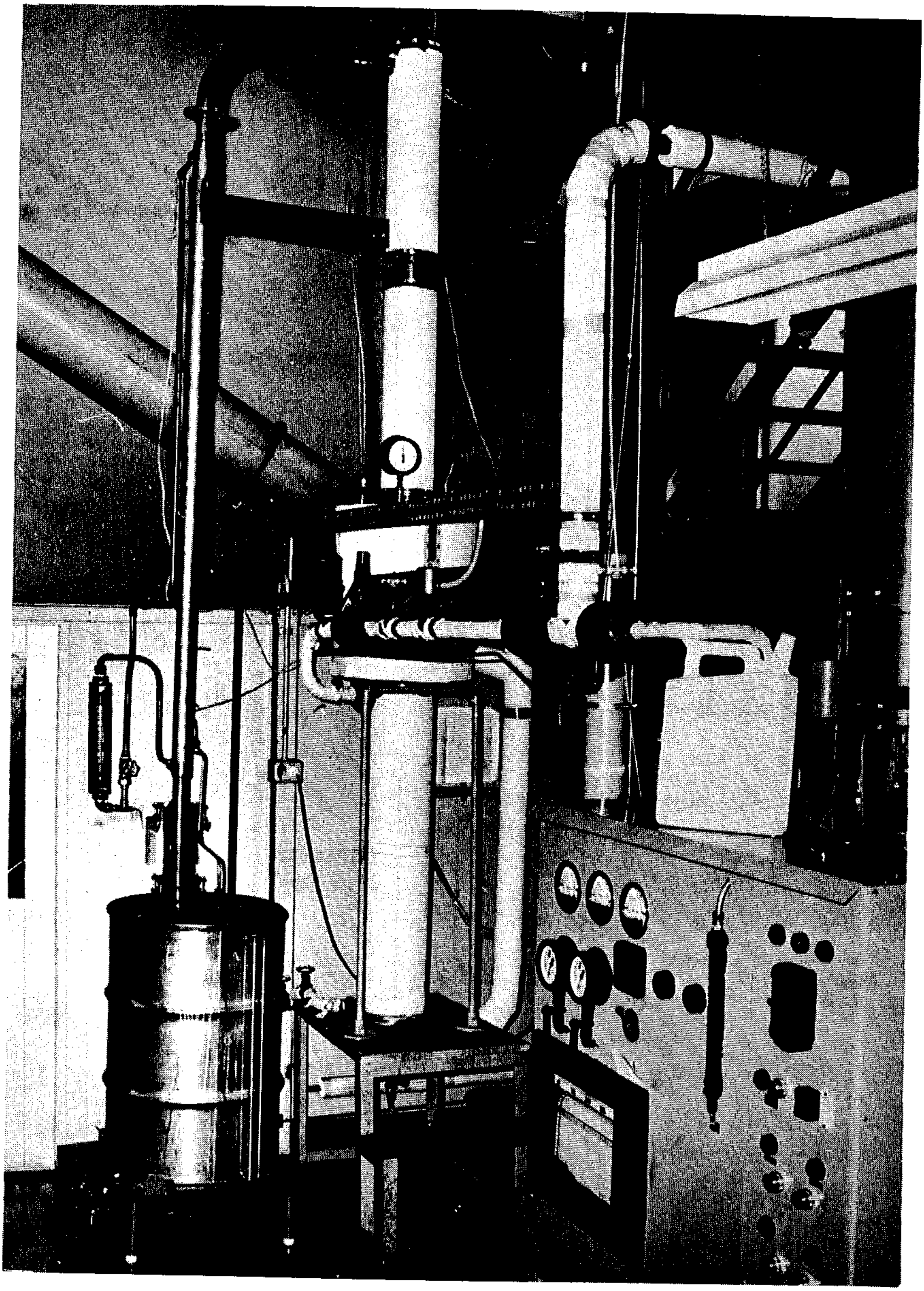

FIGURE 1. EVAPORATOR UNIT

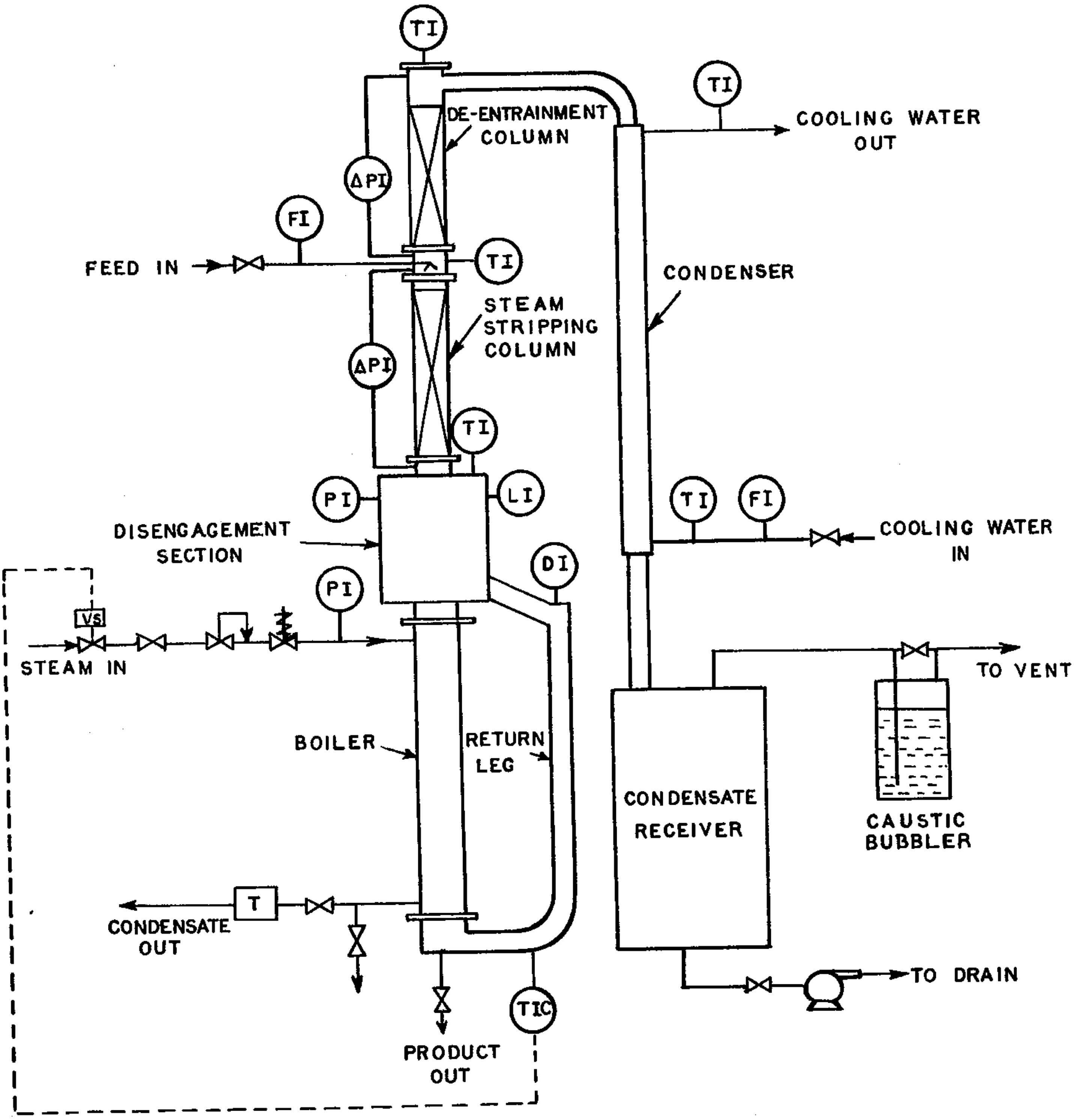

FIGURE 2. EVAPORATOR FLOWSHEET

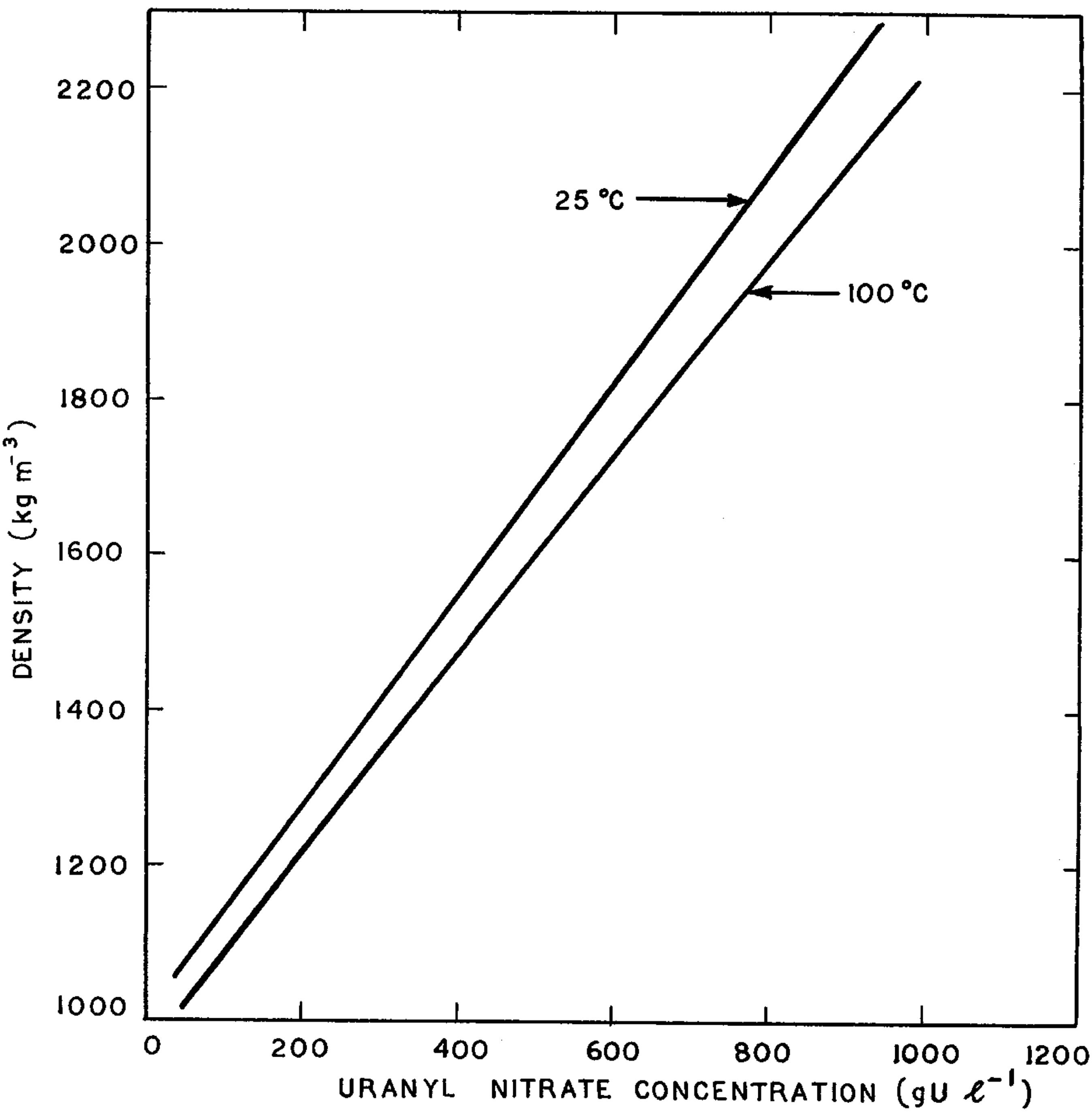

FIGURE 3. DENSITY OF URANYL NITRATE SOLUTIONS (Klitgaard et al 1964)

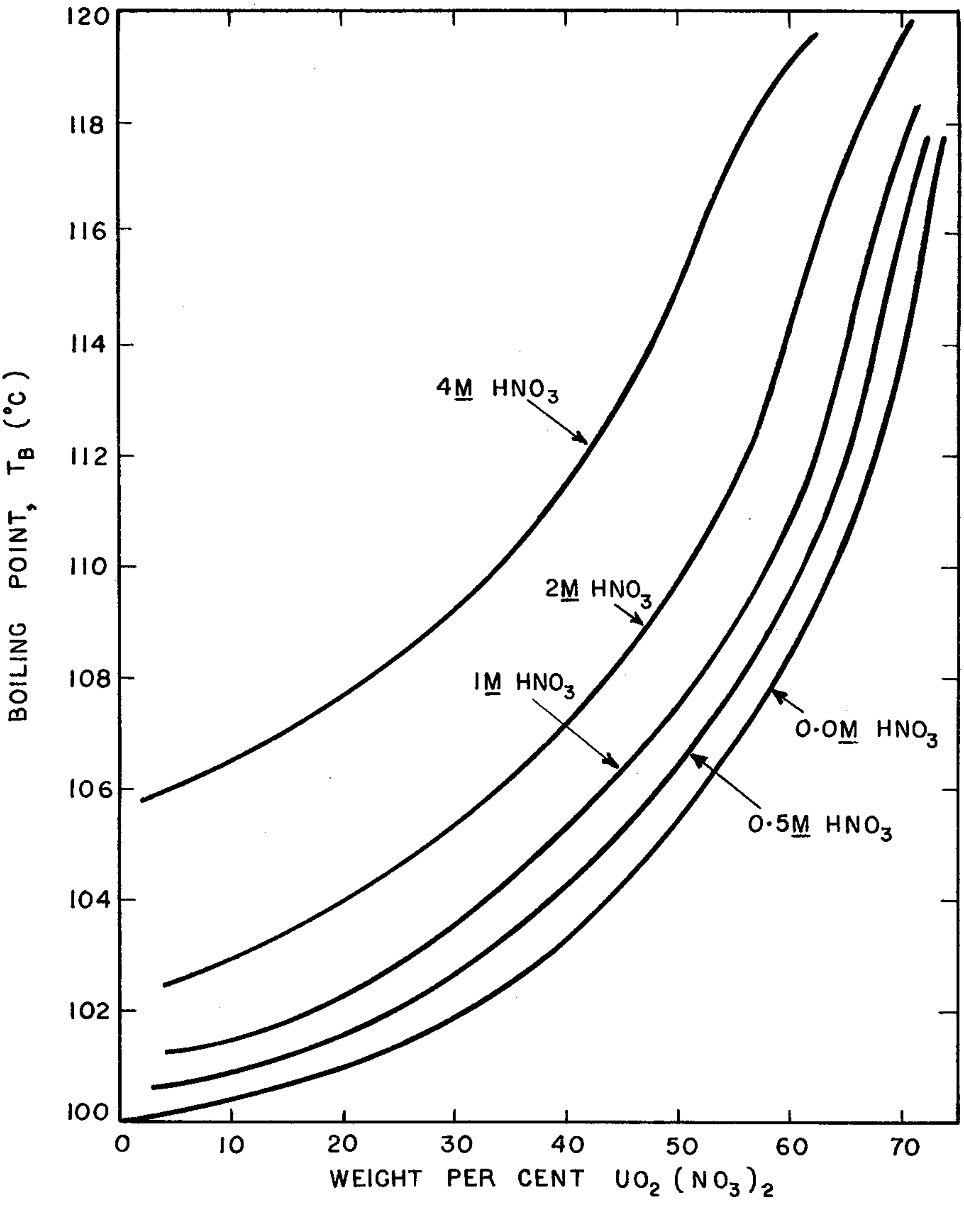

FIGURE 4. BOILING POINT OF URANYL NITRATE - NITRIC ACID SOLUTIONS

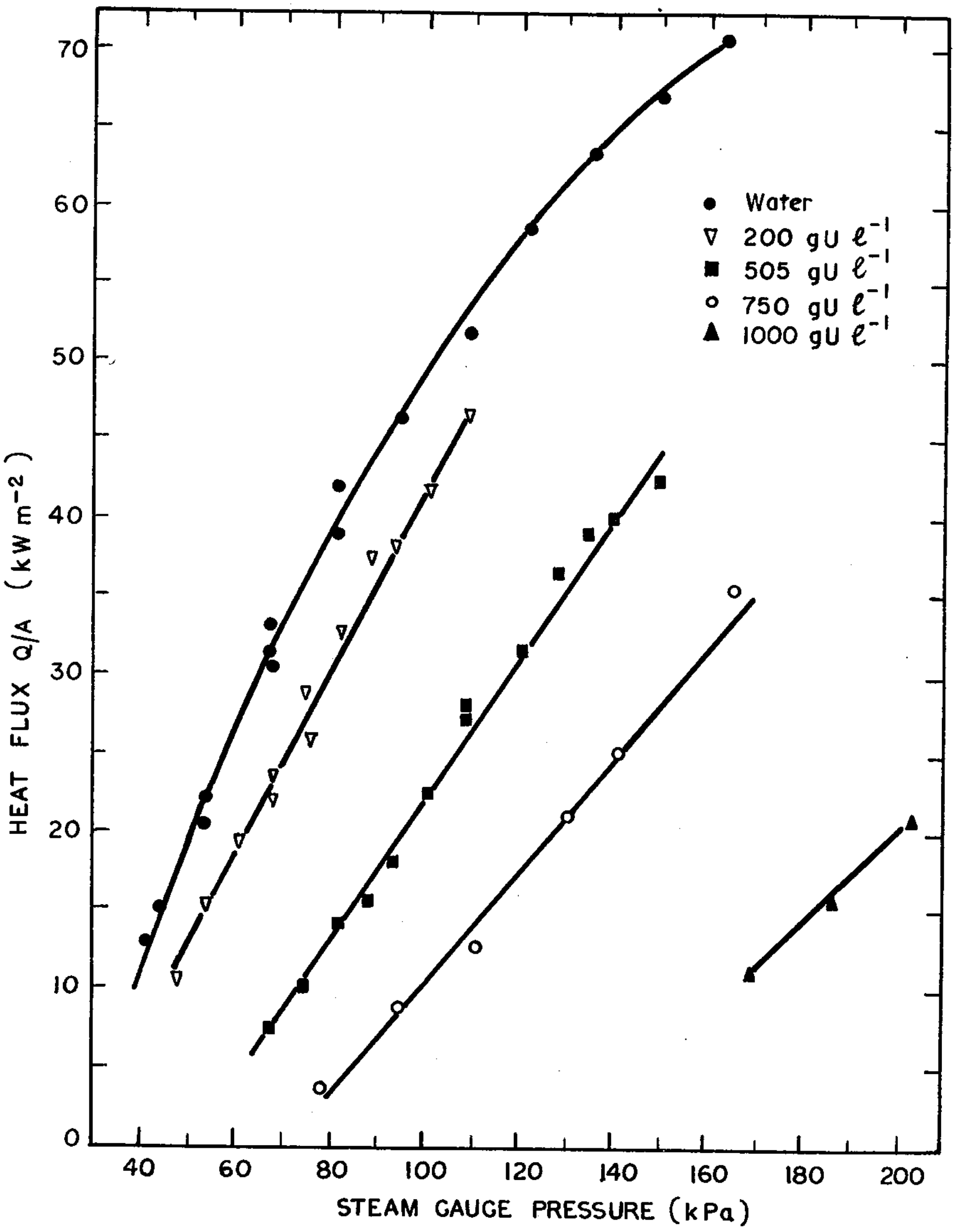

FIGURE 5. EFFECT OF STEAM PRESSURE ON HEAT FLUX

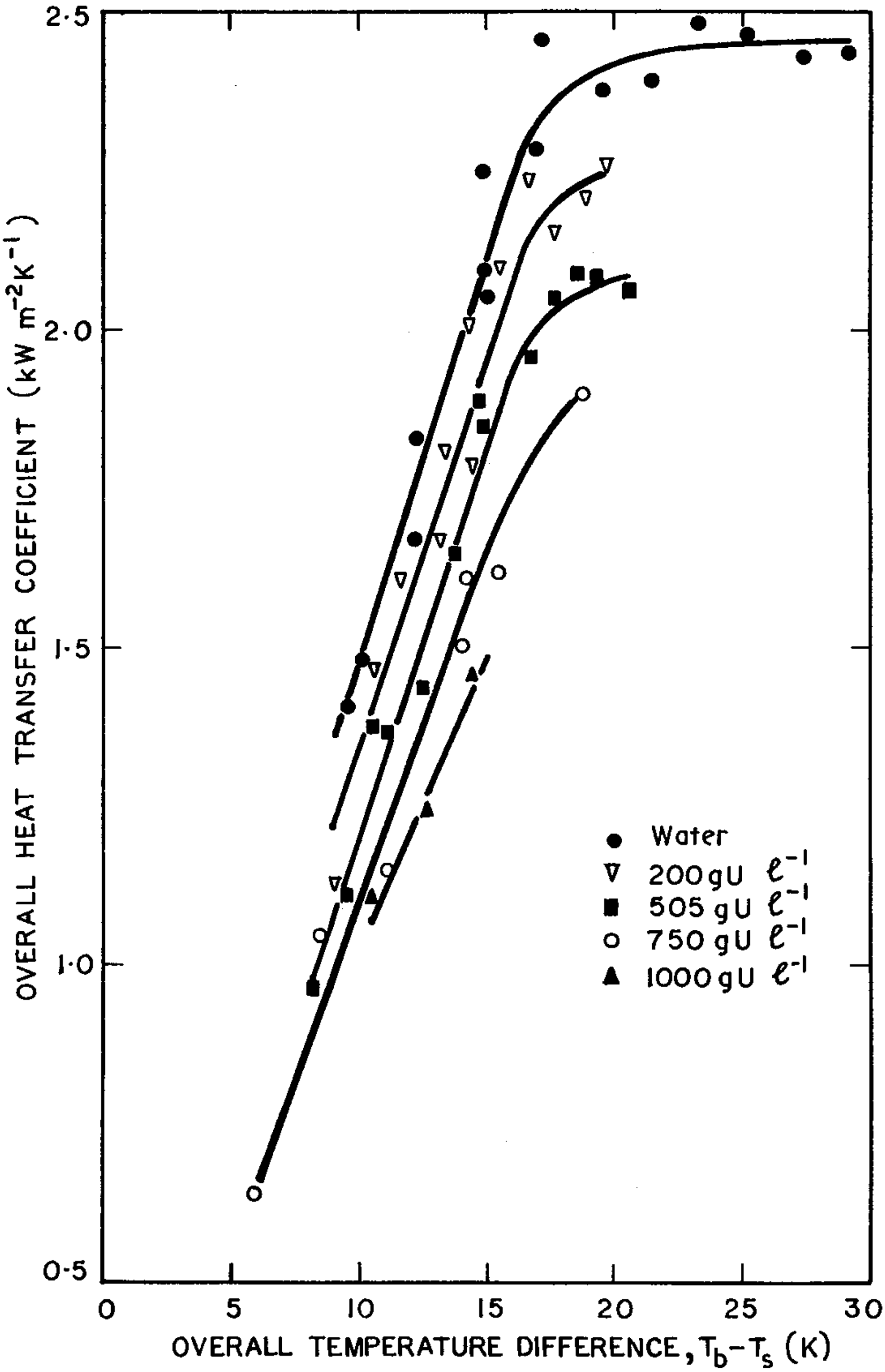

FIGURE 6. EFFECT OF OVERALL TEMPERATURE DIFFERENCE ON HEAT TRANSFER COEFFICIENT

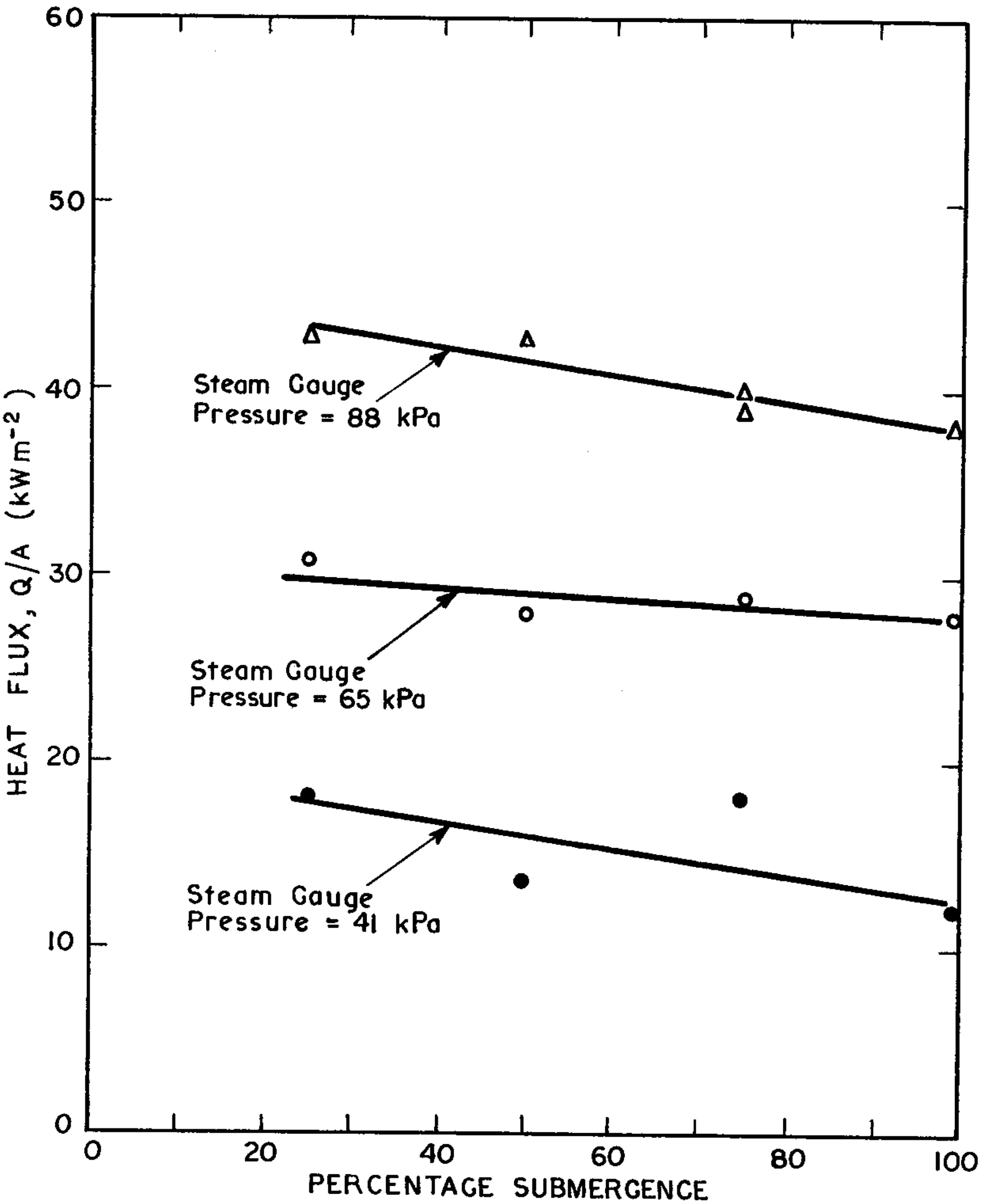

FIGURE 7. EFFECT OF LIQUID SUBMERGENCE ON EVAPORATOR PERFORMANCE

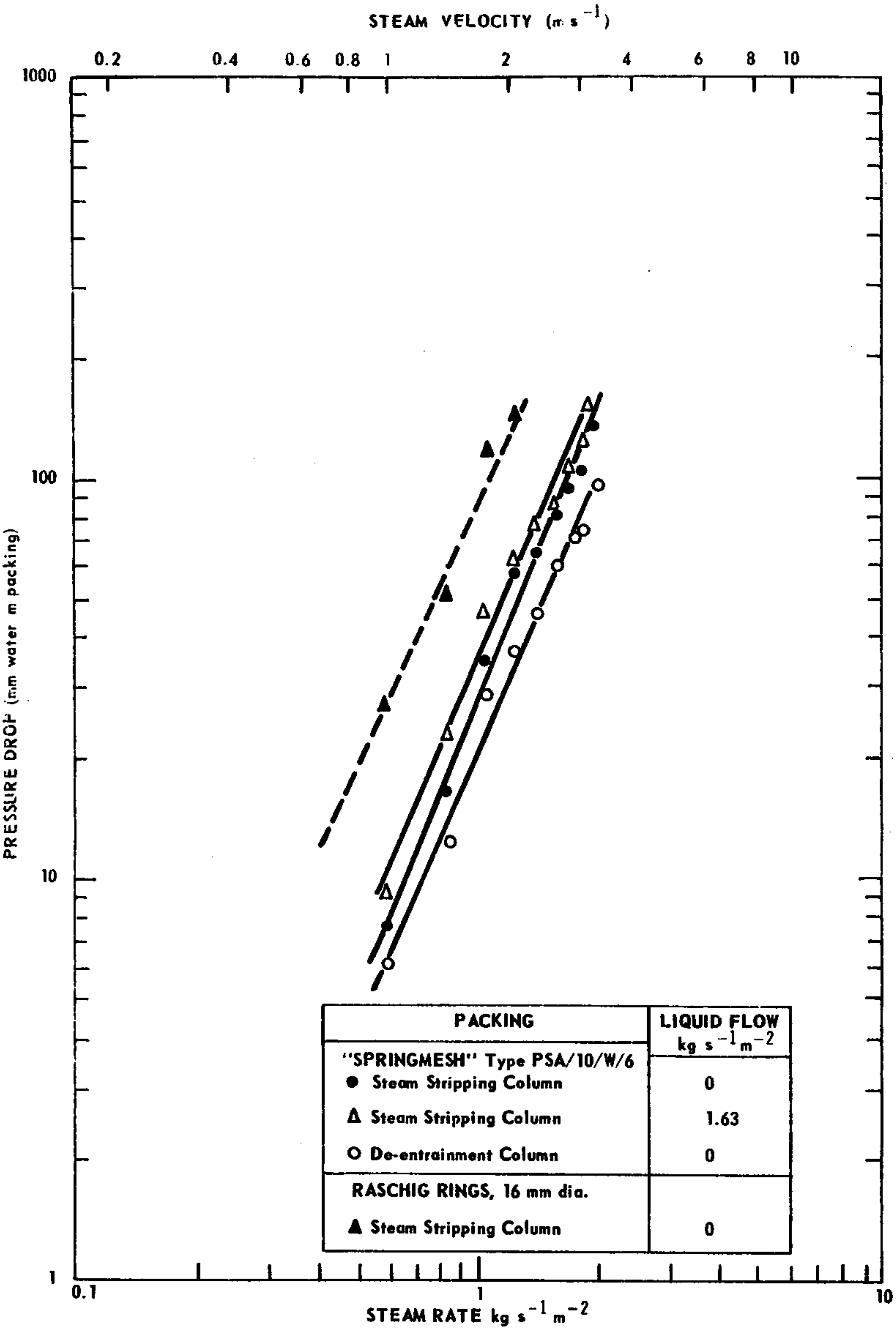

FIGURE 8. PRESSURE DROP CHARACTERISTICS OF EVAPORATOR COLUMN PACKINGS

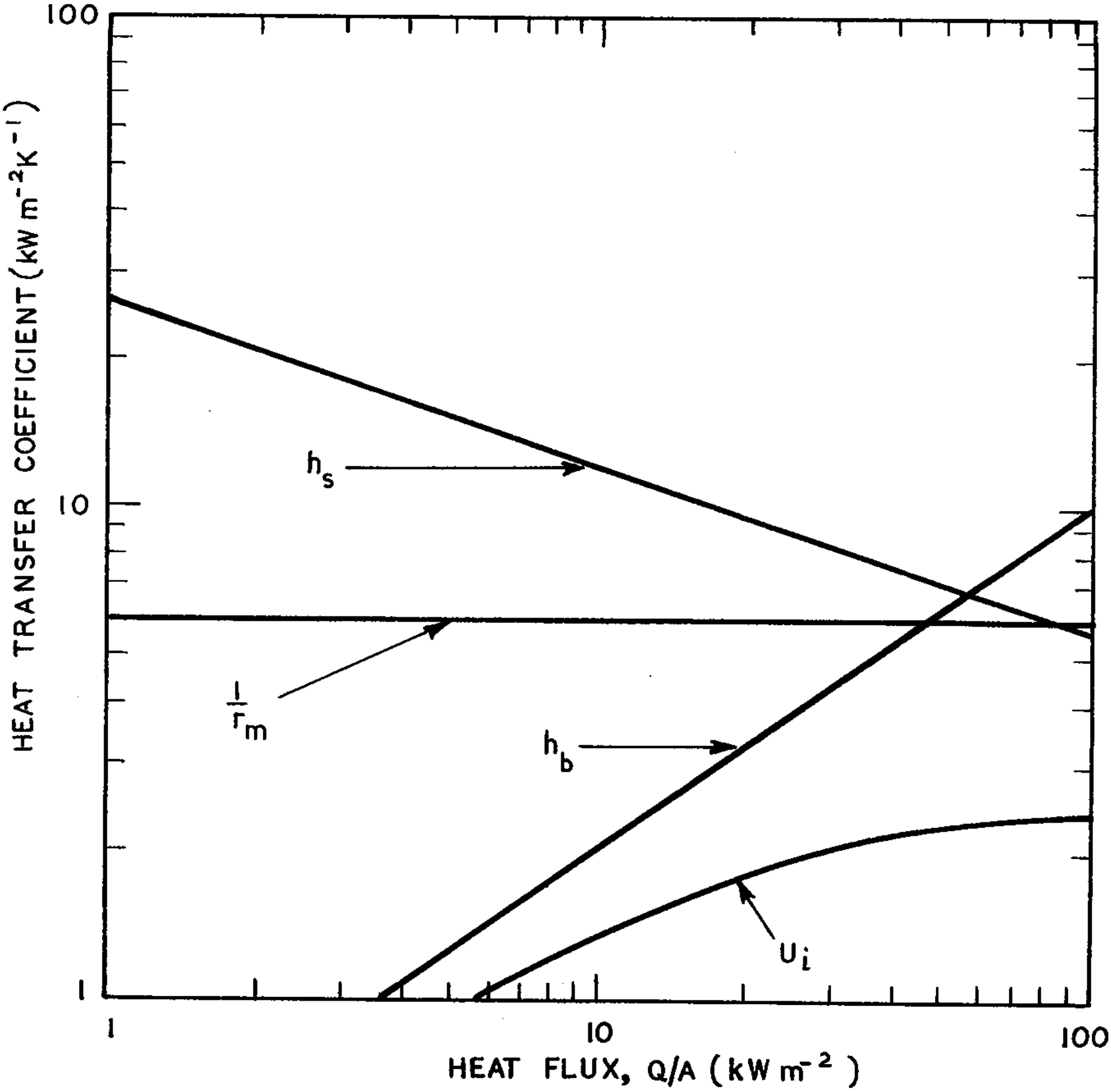

FIGURE 9. PREDICTED HEAT TRANSFER COEFFICIENTS FOR WATER

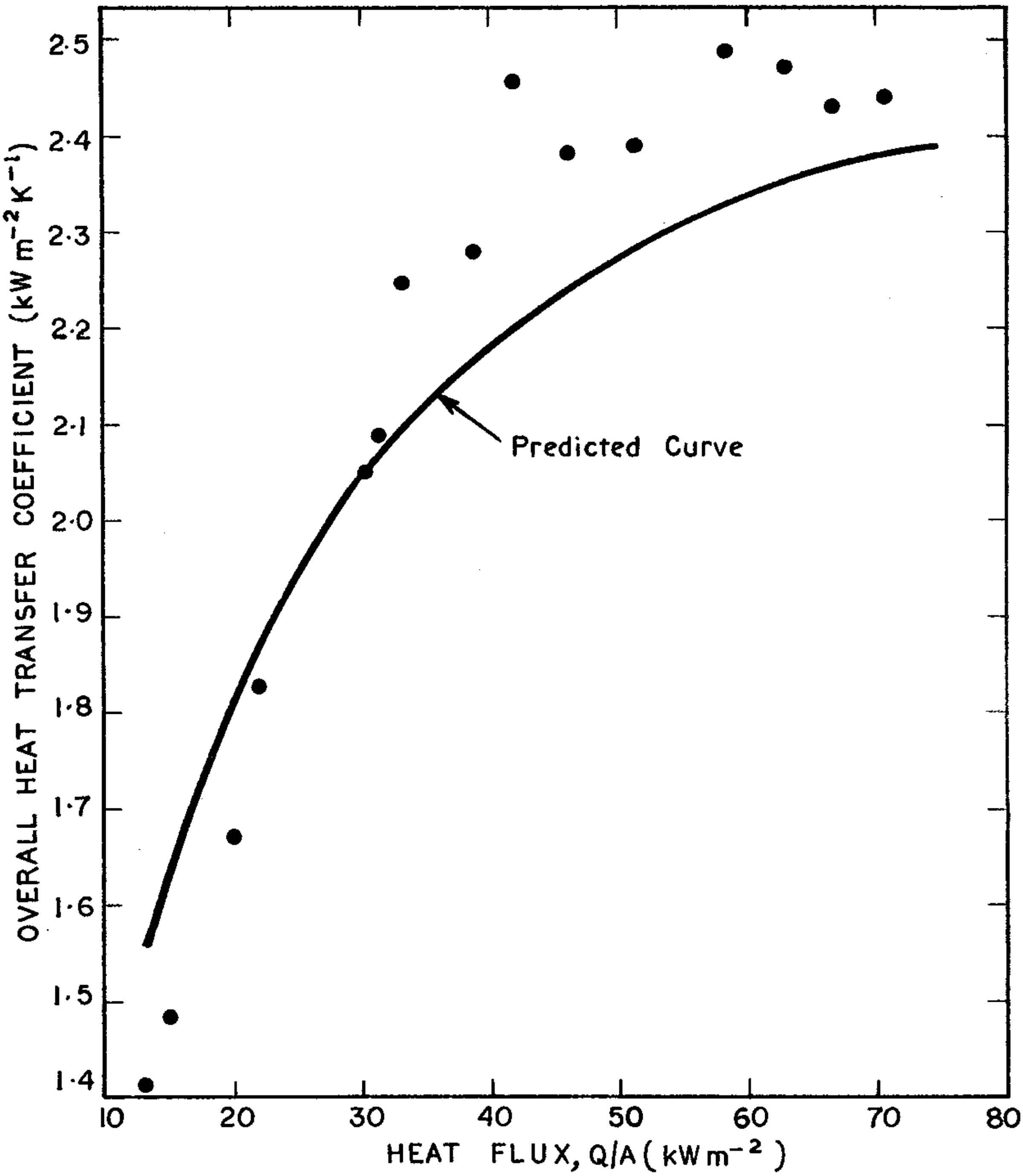

FIGURE 10. COMPARISON OF PREDICTED AND MEASURED VALUES OF U_i FOR WATER

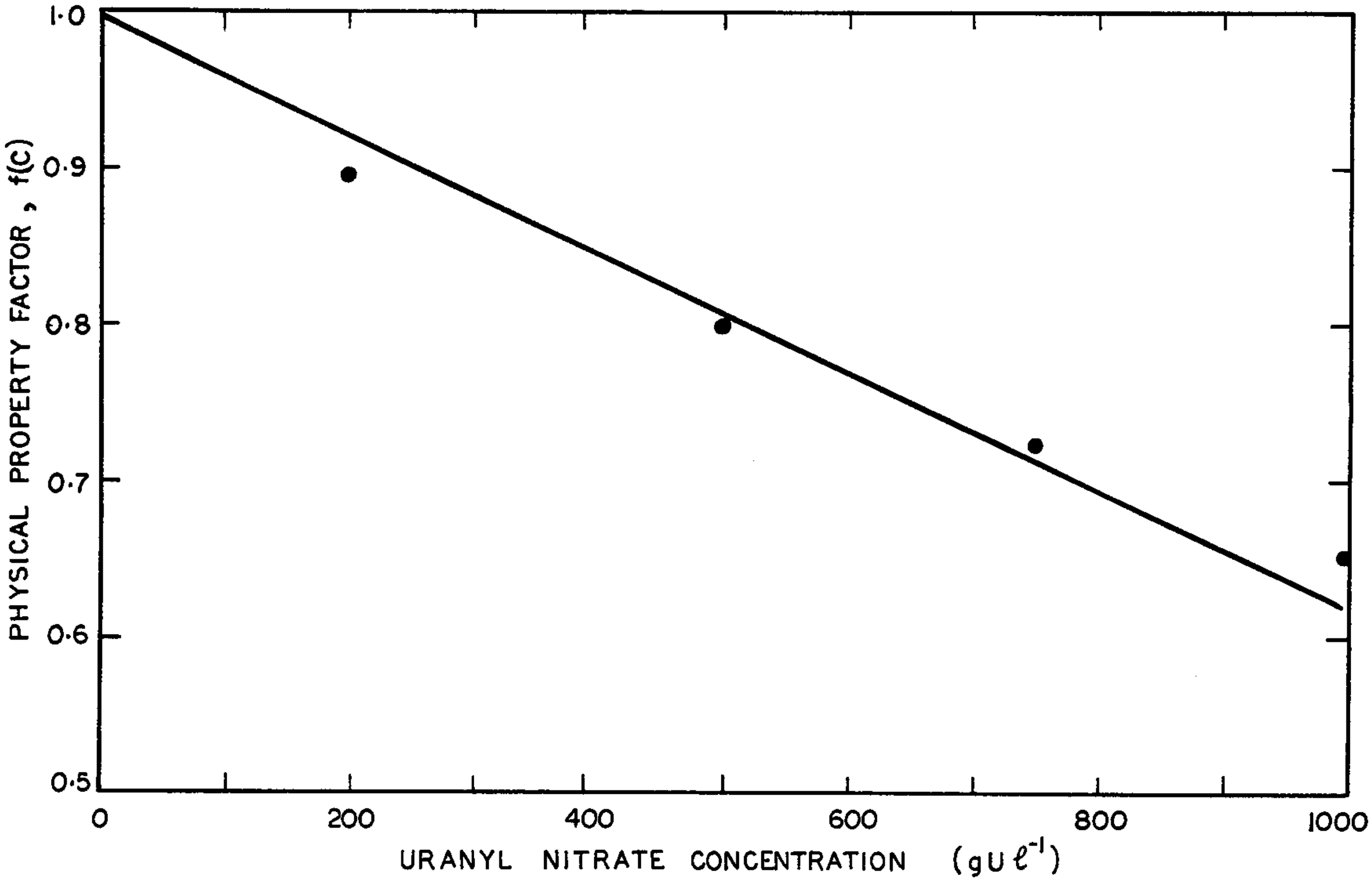

FIGURE 11. BOILING HEAT TRANSFER COEFFICIENT CORRECTION FACTOR